2008

Self-assembled deoxyguanosine based molecular electronic device on GaN substrates

H. Liddar
University of North Texas

J. Li
University of North Texas

A. Neogi
University of North Texas, arup@unt.edu

See next page for additional authors

Liddar, H., Li, J., Neogi, A., et al. Self-assembled deoxyguanosine based molecular electronic device on GaN substrates. Applied Physics Letters, 92, 013309 (2008). Copyright © 2008 AIP Publishing LLC.

Self-assembled deoxyguanosine based molecular electronic device on GaN substrates

H. Liddar, J. Li, and A. Neogi[a)]
Department of Physics, University of North Texas, Denton, Texas 76203, USA

P. B. Neogi
Department of Biology, University of North Texas, Denton, Texas 76203, USA

A. Sarkar
Michigan Molecular Institute, Midlands, Michigan 48460, USA

S. Cho and H. Morkoç
Department of Electrical and Computer Engineering, Virginia Commonwealth University, Richmond, Virginia 23284, USA

(Received 2 September 2007; accepted 3 December 2007; published online 11 January 2008)

Nanoscale hybrid molecular organic photodetectors based on self-assembled guanosine molecules conjugated to wide-bandgap GaN semiconductors has been realized in the ultraviolet wavelength regime. Metal-semiconductor-metal based photodetector is fabricated using ordering of modified guanosine based semiconductor nanowires which exhibit *I-V* characteristics with high current response and higher rectification ratio compared to Si based hybrid photodetectors. Photocurrent response of a two-terminal device shows the typical characteristics of a semiconductor photodiode with a cutoff wavelength at ~325 nm. The *I-V* characteristics have been elucidated using the induced polarization properties of self-assembled guanosine semiconductor. © *2008 American Institute of Physics*. [DOI: 10.1063/1.2828405]

Guanosine derivatives such as $dG(C_{10})_2$ deoxyguanosine molecules have been self-assembled on solid substrates such as mica, sapphire,[1,2] and even on semiconducting substrates viz. SiO_2,[3] but the effect of self-assembly on highly polar semiconductor surfaces such as GaN has not been investigated. The penetration depth of photons in silicon is low, and this makes it insensitive in vacuum ultraviolet region for application in photodetectors.[4] Silicon based photodetectors also have high dark current, and most available detectors operate in low temperature to reduce this dark current.[4] In previous studies, the polarization properies of self-assembled deoxyguanosine crystal (SAGC) in Si photodiodes has not been considered. In this study, the polarization in self-assembled wires along the direction of current flow is studied.

This work presents the fabrication of two-terminal devices from guanosine derivative based on GaN substrate that can be potentially used as a hybrid molecular based detector, rectifier, or modulator in the UV-visible region. Among the four bases of DNA, guanosine can be easily reduced to deoxyguanosine, which is commercially available. Modified guanosine has a unique sequence of groups that act as donors or acceptors of H bonds.[1,2] The conduction in guanosine molecules deposited in between metal electrodes on Si or GaN can be explained either by the direct metal—π orbital overlapping or by charge transfer via tunneling through the barrier height. Thus, the work function of the metal is an important parameter in characterizing a contact. Previous work on the work function of various metals[5–7] and DNA bases[8,9] shows that guanosine dominates the transport properties among DNA bases. The bandgap of SAGC on Si substrate is about 3.40 eV which is similar to that of GaN. Thus, this modified guanosine self-assembled on GaN is ideally suited for hybrid molecular electronic devices due to its low oxidation potential compared to other bases of DNA.[2] The lower oxidation potential favors charge transport and a strong intrinsic dipole moment of the order of 7 D, which provides a polarity to the molecules.[2]

GaN substrate has either negative or positive polarity depending upon the Ga or N ion termination at the cap layer. The surface and interface polarization results in domain formation of electronic charges.[10] The formation of domains with a specific polarity has been utilized for the enhancement of the self-assembly behavior of guanosine molecules by suitable modification of the side chains. The band gap of GaN (3.45 eV) is in the proximity of self-assembled guanosine derivative.[10,11] The transparency of GaN substrate due to wide-bandgap makes it possible to use these hybrid molecular based devices in the UV-visible region. Bow-tie-shaped electrodes used in the fabrication of the detectors orient the self-assembled guanosine molecule along an axis, in order to have a dipole moment orientation along the axis of the electrodes. Moreover, the small cross sectional area between the tips of the electrodes helps the guanosine molecule to self-assemble as the lateral periodicity of the self-assembled guanosine molecule is 2.5 nm.

A two step process is used to fabricate bow-tie-shaped electrodes [Figs. 1(a) and 1(b)]. The fabrication of bow-tie-shaped electrodes with nanometer (or larger) dimensions can be achieved using electron beam lithography. Wire bonding of electrodes for applying any bias voltage and device integration requires larger surface area ($>100\ \mu m^2$) of electrodes (as the smallest wire used in a wirebonder had a diameter of 15 μm). Thus, to optimize the fabrication process, initially larger metals pads were deposited using a metal evaporator [Fig. 1(a)]. Bow-tie-shaped electrodes of chro-

a)Electronic mail: arup@unt.edu.

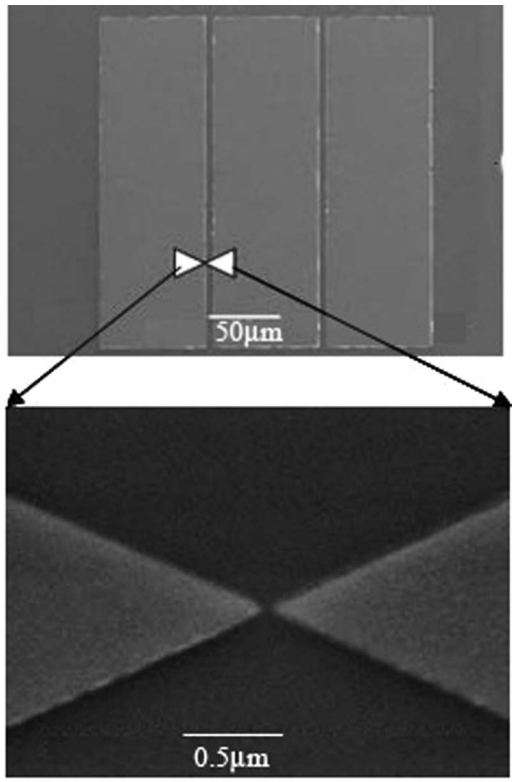

FIG. 1. Nanoscale UV photodetector integrated on a semiconductor chip. (a) Larger gold pads. (b) Magnified image of electrodes with 100 nm gate or gap.

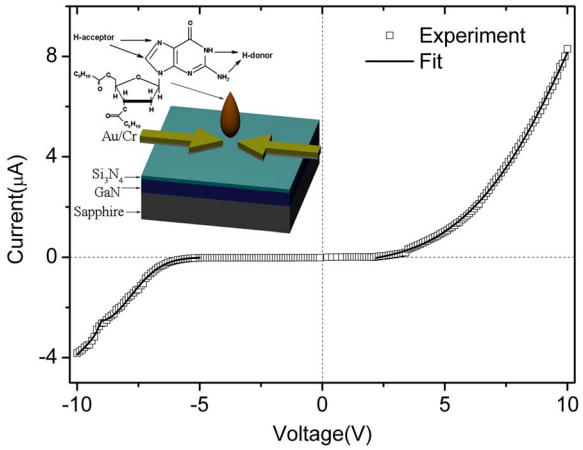

FIG. 2. Current-voltage characteristics of a two-terminal nanoscale device based on semiconductor deoxyguanosine deposited in between Au electrodes on GaN substrates. Inset is the schematic of UV-visible photodetector based on modified deoxyguanosine on GaN substrates.

mium (≈8 nm) and gold (≈30 nm) are lithographically designed on passivated GaN substrate [Fig. 1(b)]. The gap between the electrodes varies from 60 to 500 nm depending on the ordering of the guanosine wires. Devices used in the present work have 100 nm gap [Fig. 1(b)]. These electrodes were then mounted on a chip carrier and can be used as photodetectors. Thin gold wires were bonded to the gold electrodes to provide a bias voltage (±10 V).

The optimum self-assembly in between the electrodes on confined nitride nanostructure were observed by depositing a 1 μl drop of a $3.3\times10^{-3}M$ solution of $dG(C_{10})_2$ in chloroform. The protocol used to synthesize the $dG(C_{10})_2$ molecule is similar to previous reports.[1,13] The guanosine molecule was deposited in between the electrodes (Fig. 2 inset) using specially fabricated nanopipettes with a tip diameter of 100 nm. Figure 2 depicts the current voltage characteristics of the deoxyguanosine molecule under nitrogen atmosphere at room temperature. It is observed that the device shows similar characteristics to that of a metal-semiconductor-metal device. The length of the self-assembled molecular semiconductor wire in this device is ~100 nm. When a bias voltage is applied to the device, the semiconductor region is depleted and is devoid of high current flow. Metal-semiconductor-metal (MSM) structure is composed of two Schottky contacts with back-to-back alignment, as discussed by Sze *et al.*[14] The semiconductor guanosine wire connects the gold electrodes as a MSM device analogous to two Schottky diodes connected back to back. A voltage applied to the device puts one of the diodes in forward bias and another in reverse-bias condition. The leakage current is very low compared to the current flow through the self-assembled molecular wire (<200 nA). Current transport through the device is due to both majority and minority carriers. In the devised MSM structure, the current-voltage characteristics can be separated into three regions using the reach-through voltage V_{rt} and the flatband voltage V_{fb} model. If the majority carrier transport dominates, the current increases slowly with the applied voltage V. When $V>V_{rt}$, the current is proportional to $\exp(V^{1/2})$. In case of dominant minority carrier transport, the current increases gradually in the limit $V<V_{rt}$. When $V_{rt}<V<V_{fb}$, the current increases very rapidly and is proportional to $\exp(V^2)$. For V exceeding $V_{fb}(V>V_{fb})$, this increase slows down and is proportional to $\exp(V^{1/2})$. In the small voltage regime the *I-V* relation is complex and is dependent on the voltage at both contacts. The current-voltage relation can be solved numerically for $V<V_{rt}$ region and only the regions $V>V_{rt}$ has been fitted.

The band of SAGC one-dimensional wire is tilted due to the polarization induced along the axis of the ribbon-like deoxyguanosine. It results in a difference in the barrier heights and the built-in potential at two contacts. This implies that in the SAGC based MSM structure the current-voltage curves are not symmetrical. It is observed from Fig. 2 that under reverse-bias condition, the current increases very rapidly when the applied voltage is over 5 V and then slows down when it is over 9 V. This conforms to the *I-V* characteristics dominated by the minority carrier transport function with negligible contribution from majority carriers.

The current is[14]

$$I \approx I_s\left\{\exp\left[-\frac{q(V_{fb}-V)^2}{4kT(V_{fb}+\Delta\Phi_b)}\right]-\exp\left(-\frac{q\Phi_{b2}}{kT}\right)\right\}$$

when

$$V_{rt}<V<V_{fb},$$

and

$$I \approx I_s \exp\left[\frac{q}{kT}\sqrt{\frac{q(V-V_{fb})}{4\hbar\varepsilon_s L}}\right]$$

when V>Vfb, where I_s is saturation current, k is the Boltzmann constant, T is temperature, q is the electron charge, L is the thickness of the semiconductor, ε_s is the permittivity in the depletion layer, $\Delta\Phi_b$ is the built-in potential difference at two contacts, Φ_{b2} is the built-in potential at the forward-

biased contact, and $\hbar$ is Planck constant. Under forward-bias condition,

$$I(\mu A) = 16.96\{\exp[-0.023(V-15.48)^2] - 0.018\}$$

when

$$V > 2.4 \text{ V},$$

V_{rt} is estimated to be 2.4 V from Fig. 2.

While under reverse-bias condition,

$$I(\mu A) = 2.54 \exp[-0.31(V-9.08)^2],$$

when

$$5 \text{ V} < V < 9.08 \text{ V},$$

where V_{rt} is estimated to be 5 V from Fig. 2, and

$$I(\mu A) = 2.54 \exp(0.44\sqrt{V-9.08})$$

when

$$V > 9.08 \text{ V}.$$

The difference of V_{fb} under forward- and reverse-biased conditions is possibly caused by effects other than Schottky effect, the origin of which is still not clear. The saturation current depends on the barrier height of Schottky contact. The different saturation currents imply the different barrier height at two contacts. As the curve fit satisfactorily with the minority carrier transport, it implies a lower barrier height for minority charge carriers compared to the majority carriers.

It is also observed that there is no significant difference in the *I-V* characteristics under room and dark condition. In the low current region, electrons having energy greater than the barrier height cross the barrier and enter the semiconductor region and result in current flow across the junction. As the applied bias voltage increases, the barrier height decreases making it easier for the electrons to cross the barrier.

The dynamic resistance can be found from the derivation of current–voltage equations. Under forward-bias condition, the dynamic resistance increases monotonically from 1.9 kΩ at 2.4 V to 117.1 kΩ at 10 V. Under reverse-bias condition, the dynamic resistance increases monotonically in the range $5 \text{ V} < V < 9.08$ V. At 5 V, it is 0.89 kΩ. It increases rapidly as the applied voltage approaches 9.08 V. The dynamic resistance increases monotonically in the range $9.08 \text{ V} < V \leqslant 10$ V. It is close to 0 when the applied voltage is close to 9.08 V. It is 1.13 MΩ at 10 V. The MSM structure has capacitance in the depletion layer, just like in *p-n* junction. The capacitance decreases slowly as minority carrier current increases. The smaller resistance implies a faster response time. The dynamic resistance can be significantly reduced by long range ordering of the molecular wires and appropriate surface modification of the substrate. The figure of merit of device estimated from the rectification ratio in GaN based system is significantly higher than Si based hybrid photodiodes.

Figure 3 represents the photocurrent spectrum of a two-terminal device in inert atmosphere under dark conditions which was measured using a Xe-lamp source and a monochromator. The photocurrent spectrum is typical of a semiconductor photodiode and shows an absorption bandedge at ~320 nm. For a similar concentration of the SAGC molecule a 20 nm blueshift of the cutoff wavelength toward the UV wavelength is observed compared to Si based SAGC system.[3] The absorption edge of the SAGC wires are observed to be at a higher energy compared to the bulk GaN bandedge. Our recent results also show that the long range ordering of the self-assembled wires and consequently the gap length between the electrodes can be enhanced to 500 nm to enable photolithography techniques.

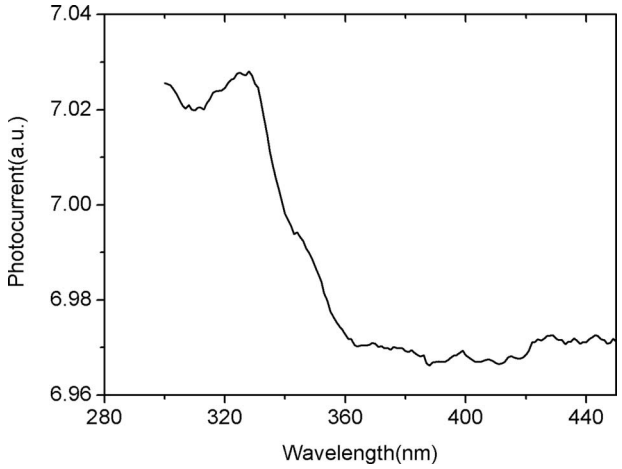

FIG. 3. Photocurrent spectrum of SAGC based photodiode exhibiting semiconducting behavior.

In conclusion, self-assembled guanosine based molecular wires have been used to fabricate two-terminal diode on GaN semiconductor substrates. Due to polarity induced along the direction of the SAGC wires during the self assembly process, the output current of the GaN based photodiodes is significantly higher than hybrid Si-self-assembled oligonucleotide based photodiodes at similar input voltage. The cutoff wavelength can be reduced to ~325 nm.

This work is supported by National Science Foundation under Grant No. ECS-05-33960 entitled "Self-assembled guanosine based hybrid single-molecular electronic devices."

[1] G. Gorrarelli, S. Masiero, E. Mezzina, S. Pieraccini, J. P. Pabe, P. Samorí, and G. P. Spada, Chem.-Eur. J. **6**, 3242 (2000).
[2] G. Maruccio, P. Visconti, V. Arima, S. D'Amico, A. Biasco, E. D'Amone, R. Cingolani, and R. Rinaldi, Nano Lett. **3**, 479 (2003).
[3] R. Rinaldi, G. Maruccio, A. Biasco, V. Arima, R. Cingolani, T. Giorgi, S. Masiero, G. P. Spada, and G. Gottarelli, Nanotechnology **13**, 398 (2002).
[4] U. Schüehle, J.-F. E. Hochedez, J. L. Pau, C. Rivera, E. Muñoz, J. Alvarez, J.-P. Kleider, P. Lemaire, T. Appourchaux, B. Fleck, A. Peacock, M. Richter, U. Kroth, A. Gottwald, M.-C. Castex, A. Deneuville, P. Muret, M. Nesladek, F. Omnes, J. John, and C. Van Hoof, Proc. SPIE **5171**, 231 (2004).
[5] C. D. Hodgman and W. R. Veazey, *Handbook of Chemistry and Physics*, 47th ed. (Chemical Rubber, Cleveland, 1996), p. E-68.
[6] N. W. Ashcroft and N. D. Mermim, *Solid State Physics* (Saunders College, Philadelphia, 1976), p. 364.
[7] G. M. Barrow, *Physical Chemistry*, 5th ed. (McGraw-Hill, New York, 1988), p. 581.
[8] H. Sugiyama and I. Saito, J. Am. Chem. Soc. **118**, 7063 (1996).
[9] S. D. Wetmore, R. J. Boyd, and L. A. Eriksson, Chem. Phys. Lett. **322**, 129 (2000).
[10] D. Huang, M. A. Reschikov, and H. Morkoç, Int. J. High Speed Electron. Syst. **12**, 79 (2002).
[11] A. Neogi, H. Morkoc, T. Kuroda, and A. Tackeuchi, IEEE Trans. Nanotechnol. **2**, 10 (2003).
[12] A. Neogi, J. Li, P. B. Neogi, A. Sarkar, and H. Morkoc, Electron. Lett. **40**, 1605 (2004).
[13] L. H. Koole, H. M. Moody, N. L. H. L. Broders, P. J. L. M. Quaedflieg, W. H. A. Kuijpers, M. H. P. van Genderen, A. J. J. M. Coenen, S. van der Wal, and H. M. Buck, J. Org. Chem. **54**, 1657 (1989).
[14] S. M. Sze, D. J. Coleman, and A. Lya, Solid-State Electron. **14**, 1209 (1971).